



Article

A Na⁺/H⁺ Antiporter Gene from *Rosa multiflora* (*RmNHX2*) Functions in Salt Tolerance via Modulating ROS Levels and Ion Homeostasis

Haiyan Luo ^{1,†} , Yuxiao Shen ^{2,†}, Linmei Chen ¹, Yongyi Cui ¹ and Ping Luo ^{1,*}

¹ College of Horticulture Science, Collaborative Innovation Center for Efficient and Green Production of Agriculture in Zhejiang Mountainous, Zhejiang A & F University, Hangzhou 311300, China

² College of Landscape Architecture and Art, Henan Agricultural University, Zhengzhou 450002, China

* Correspondence: pingluo@zafu.edu.cn

† These authors contributed equally to this work.

Abstract: High salinity restricts plant growth and geographic distribution. Plant intracellular Na⁺/H⁺ (NHX) antiporters have critical roles in plant development and stress response. However, the molecular functions of *RmNHXs* in *Rosa multiflora* remain unclear. In this study, we identified 11 putative *RmNHXs* in *R. multiflora* according to the genome-wide analysis. The *RmNHXs* were classified into three classes. Most of the *RmNHXs* were responsive to salt stress, with the greatest upregulation being observed in *RmNHX2*. *RmNHX2* was localized at the tonoplast. *RmNHX2* overexpression resulted in the enhanced salt tolerance in tobacco, whereas virus-induced gene silencing (VIGS) of *RmNHX2* in *R. multiflora* elevated salt susceptibility. Under salt treatment, the transgenic tobaccos achieved less reactive oxygen species (ROS) accumulation and higher activities of antioxidant enzymes, which complied with the upregulated expressions of antioxidant genes. Moreover, *RmNHX2*-overexpression lines had a lower level of Na⁺, a higher level of K⁺, and a lower Na/K ratio. In contrast to the mentioned, VIGS of *RmNHX2* in *R. multiflora* exhibited the opposite phenotype, accompanied by a compromised salt tolerance. Regarded together, these results demonstrate that *RmNHX2* enhances plant salt tolerance by maintaining proper ion homeostasis, as well as by accelerating ROS scavenging.

Keywords: *Rosa multiflora*; *RmNHX2*; salt tolerance; ion homeostasis; ROS scavenging



Citation: Luo, H.; Shen, Y.; Chen, L.; Cui, Y.; Luo, P. A Na⁺/H⁺ Antiporter Gene from *Rosa multiflora* (*RmNHX2*) Functions in Salt Tolerance via Modulating ROS Levels and Ion Homeostasis. *Horticulturae* **2023**, *9*, 290. <https://doi.org/10.3390/horticulturae9030290>

Academic Editor: Simone Landi

Received: 1 December 2022

Revised: 6 February 2023

Accepted: 10 February 2023

Published: 21 February 2023



Copyright: © 2023 by the authors. Licensee MDPI, Basel, Switzerland. This article is an open access article distributed under the terms and conditions of the Creative Commons Attribution (CC BY) license (<https://creativecommons.org/licenses/by/4.0/>).

1. Introduction

Abiotic stresses involve environment conditions (e.g., salt injury, extreme temperature, and drought) that severely affect the quantity and quality of crop products. Salt stress is a major stress-depressing plant growing process, limits crop production, and is a great threat to agricultural development all over the world [1]. Moreover, fertilization and irrigation could cause secondary soil salinity [2]. In addition, salinity can destroy physio-biochemical function and cause the death of plant cells and plants itself via osmotic stress, ion toxicity, and nutrition imbalance attributed to the excess of Na⁺ and Cl⁻ [3]. Accordingly, analyzing the mechanism underlying plant responses to salt stress and exploring salt tolerance-related genes can theoretically and practically help.

To address soil salinity, plants have developed several adaptive mechanisms that are crucial for the survival of plants [4]. Plants are capable of perceiving the salt stress signals from their cellular, physiological, and biochemical responses, transmitting the signals as well as regulating the expression of related genes to respond to salinity [5]. For instance, plants could control the loss of water to alleviate salt damage via regulating the closure of the stomata [6]. Over the past few decades, it was extensively demonstrated that salt tolerant related genes can be classified into two groups in accordance with their function. The former group's function is protecting cells against damage derived from salt stress [7].

Transcription factors (TFs), protein phosphatases, and protein kinases, i.e., the second group, are critical to stress signal transduction and stress-responsive gene activation [8]. As genetic engineering leaps forward, horticultural crops can be advanced at the gene level and increase the resistance ability [9]. Abiotic stresses also led to the accumulation of ROS, including hydrogen peroxide (H_2O_2) and hydroxyl radicals, O_2^- (superoxide radicals), in plant cells [10]. ROS scavenging enzymes are responsible for protection against oxidative damages on cell membranes [10]. Furthermore, given that, it will be of high significance for exploiting the favorable genes to increase the salt tolerance of plants.

Plants have evolved several defense systems (e.g., ion efflux from cells and sequestration) to adapt to the salt stress [11]. The plant sodium-proton antiporters (NHXs) were initially demonstrated to have a mediating effect on the electroneutral Na^+/H^+ exchanging process, sequestering excess cytosolic Na^+ to the vacuole and maintaining ionic equilibrium [12]. It was reported that there are eight NHX members in *Arabidopsis* [13]. According to the sequence similarity and localization, the NHXs of *Arabidopsis* fall to three distinct classes, i.e., the plasma membrane-located AtNHX7/8, endosome-located AtNHX5/6, and vacuolar membrane-located AtNHX1/2/3/4 [14]. It is noteworthy that the vacuolar and plasma membrane-located NHXs in *Arabidopsis* critically impact the salt tolerance through the maintenance of Na^+/K^+ homeostasis [15]. The heterologous expression of two NHXs (*HtNHX1* and *HtNHX2*) from a salt-tolerant plant *Helianthus tuberosus* increased the salt tolerance of rice [16]. In *Pyrus ussuriensis*, the overexpression of *PbrNHX2*, located in the tonoplast, enhanced salt tolerance by maintaining a high K^+/Na^+ ratio [17]. The mentioned results indicated that the NHXs proteins positively impacted plants' salt tolerance. It is critical to isolate and characterize the function of NHXs in plants.

The *Rosa multiflora* Thunb, as a root stock for the modern rose (*Rosa hybrida*), is a cold and salt tolerant genotype; thus, the functional identification of salt-tolerant genes would substantially benefit from the genetic breeding of roses. This study characterized *RmNHX2* from *R. multiflora*. *RmNHX2* overexpression in tobacco increased the salt tolerance, whereas the downregulation of *RmNHX2* in *R. multiflora* using VIGS led to the improved salt sensitivity as well. As revealed from the results here, the *RmNHX2* could potentially be employed in the improvement of subsequent rose salt tolerance.

2. Results

2.1. Identification of *RmNHXs* in *Rosa multiflora*

A total of 11 NHXs in *R. multiflora* was obtained according to the genome-wide analysis (Figure 1A). The basic parameters about these *RmNHXs* were exhibited in Table S1, including gene ID, coding sequence (CDS) length, molecular weight (Mw), and isoelectric point (pI). As presented in Table S1, the *RmNHXs* varied from 268 to 695 aa in size with pI being between 5.03 and 9.03 and MW being between 29.47 and 62.51 kD. In addition, the phylogenetic analysis was performed based on the *RmNHXs* and NHXs from other plant species, which could be classified as vacuolar (Class I), endosomal (Class II), and plasma membrane types (Class III) (Figure 1A). Nine *RmNHXs* were categorized in Class I, one in Class II, and one in Class III, respectively (Figure 1B).

The intron-exon structure analysis was conducted in the conserved Na^+/H^+ exchanger domains of the *RmNHXs* (Figure 2A). As shown in Figure 2A, the gene structure of 11 *RmNHXs* showed diverse intron-exon patterns with the number of introns ranging from 7 to 24. On the other hand, the longest intron of *RmNHX2* is 2.9 kb. As a result, the genome sequences of *RmNHX2* reached 7.8 kb (Figure 2B). These data revealed that the changes of the gene structure in *RmNHXs* might lead to their function divergences during the evolution.

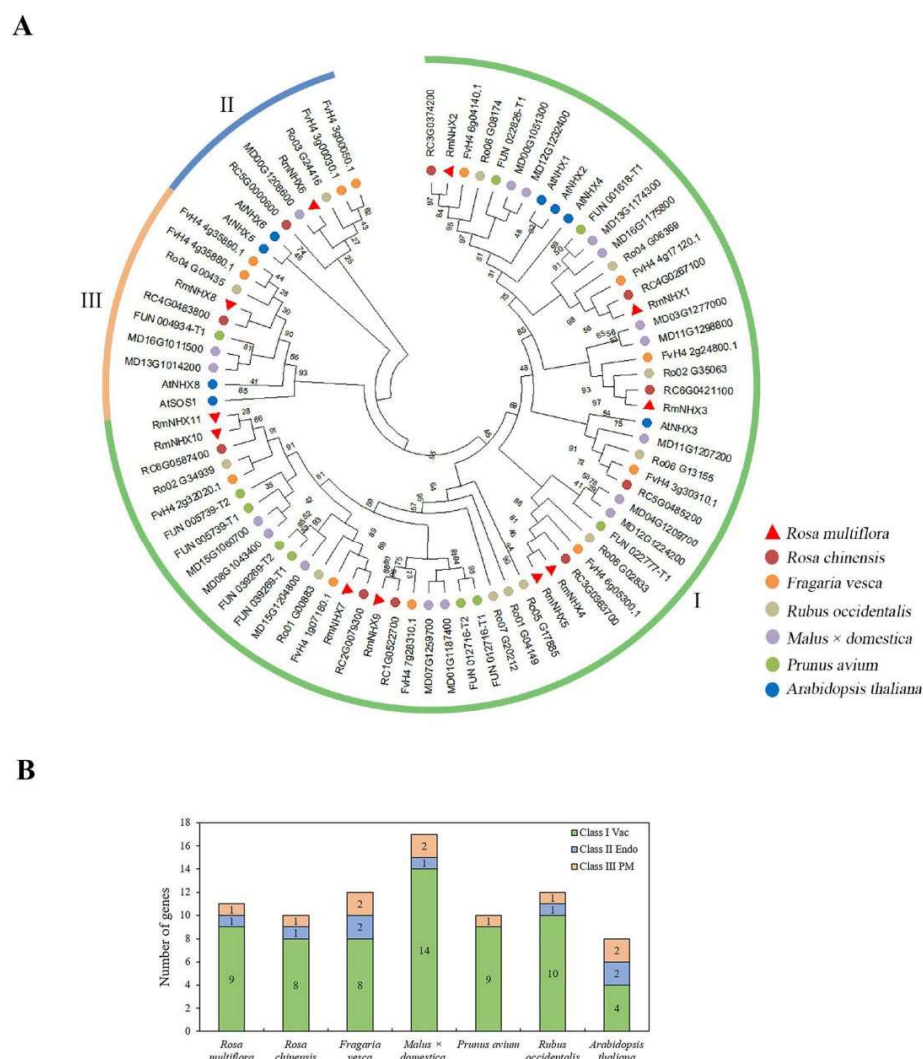


Figure 1. Phylogenetic tree analysis of NHX gene family. **(A)** Phylogenetic clustering of from wild rose, rosa, strawberry, apple, cherry, raspberry, and *Arabidopsis*. MEGA 7 was used to construct the phylogenetic tree using the NJ method. The proteins were clustered into three groups. Different background colors indicate the different group of the NHXs proteins. **(B)** The number of three types NHX gene in wild rose, rosa, strawberry, apple, cherry, raspberry, and *Arabidopsis*.

To gain insights into the function of *RmNHXs*, the 2.0 kb promoter region of the *RmNHXs* was adopted to identify the cis-acting elements using the PlantCARE database. According to Figure S1, the promoter region of *RmNHXs* had various cis-acting elements (e.g., CAAT-box, CCAAT-box, and TATA-box), thereby demonstrating that the *RmNHXs* are closely related to plant growth and development. Moreover, plant hormone-responsive and stress-responsive elements were also identified in the promoter region of *RmNHXs*, including salicylic acid responsive elements (TCA-elements), auxin responsive elements (TGA-elements), MeJA-responsive elements (CGTCA-motif and TGACG-motif), ABA responsive elements (ABREs), gibberellin-responsive elements (TATC-box), low-temperature responsive elements (LTR), and defense and stress responsiveness elements (TC-rich repeats) (Figure S1). It should be noticed that there were different number of hormone and stress response motifs in the promoter region of *RmNHXs* (Figure 2C). These results indicated that *RmNHXs* might have different roles in hormone and stress responses.

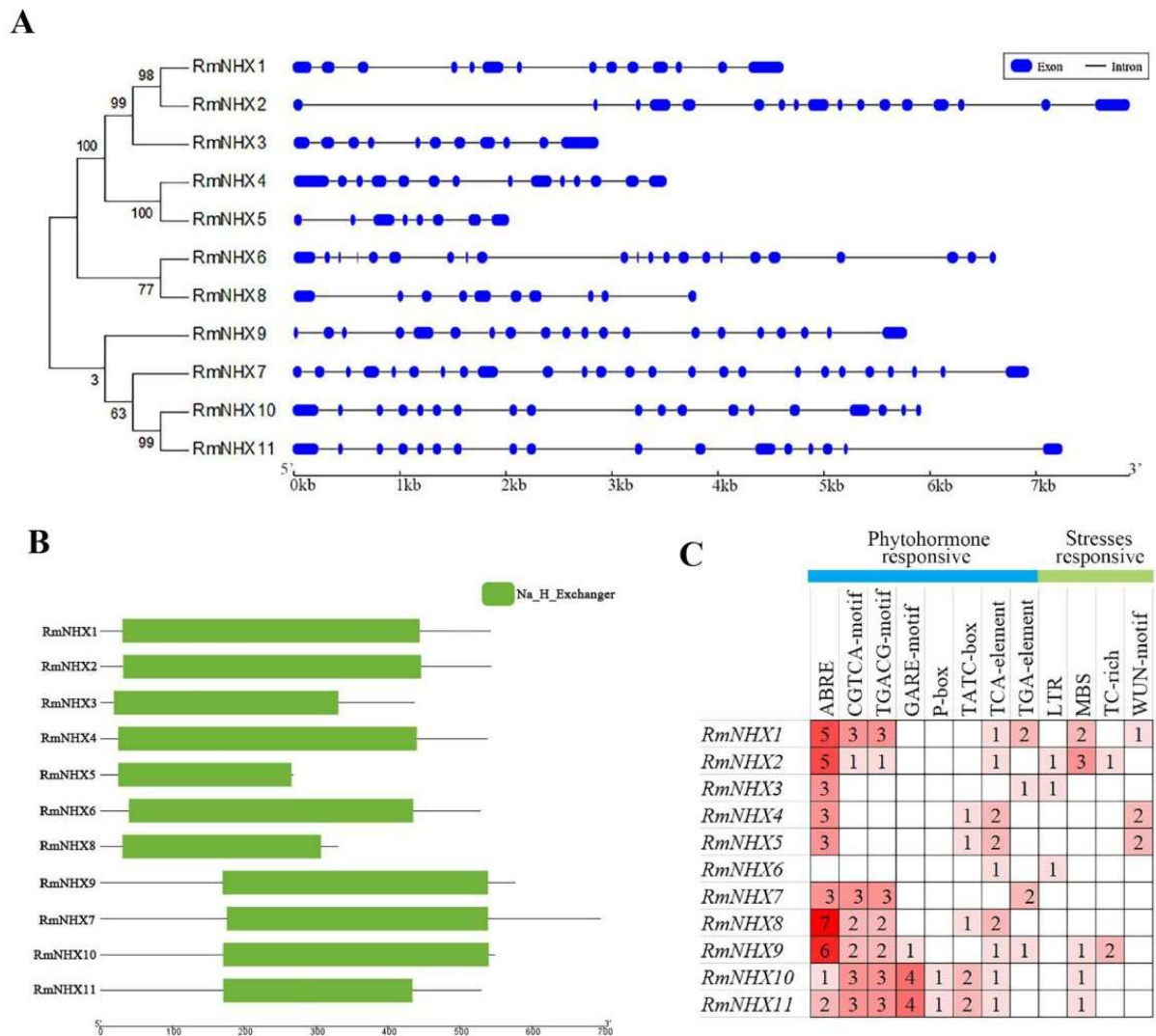


Figure 2. The conserved motifs and gene structure analysis of *RmNHX* gene family in wild rose. (A) Gene structure analysis of *RmNHXs*. Exons are represented by boxes, while introns are represented by gray lines. The cis-acting elements are indicated in different colored boxes. (B) Conserved motif analysis of *RmNHXs*. Na^+/H^+ exchanger domain is marked in green. (C) Promoter analysis of cis-acting regulatory elements related to stress response in *RmNHXs*. The different number and color stand for the number of cis-elements in the *RmNHXs* promoters.

2.2. Expression Pattern and Subcellular Localization of *RmNHXs*

To further explore the potential functions of *RmNHXs*, we conducted quantitative real-time PCR (qRT-PCR) to assess the expression pattern of *RmNHXs* in response to salt stress. When subjected to salt stress, most of *RmNHXs* showed an alteration of expression levels, while the expression pattern of each *RmNHXs* was different, demonstrating the differences in the potential roles of *RmNHXs* under salt response (Figure 3a). Among them, the expression level of *RmNHX2* was drastically upregulated by the salt treatment (Figure 3a). The *RmNHX2* expression efficiently increased in 0.5 h in response to salt stress and it reached the maximum expression in 5 h (about 6.8-fold), followed by gradually declining until the last time point (48 h) (Figure 3a). As shown in Figure 3b, *RmNHX2* expression efficiently increased in 0.5 h in response to dehydration, after which it began to decline. When subjected to cold stress, the expressing state of *RmNHX2* did not noticeably change, suggesting that *RmNHX2* was not cold-inducible (Figure 3b). In the case of exogenous ABA treatment, *RmNHX2* mRNAs initially remained steady at 1 h and then elevated by 2.2-fold

at 12 h (Figure 3b). Compared with dehydration and ABA, the salt treatment caused a greater induction, indicating that *RmNHX2* might impact plant abiotic stress resistance, especially salt. The *RmNHX2* was chosen for further function analysis.

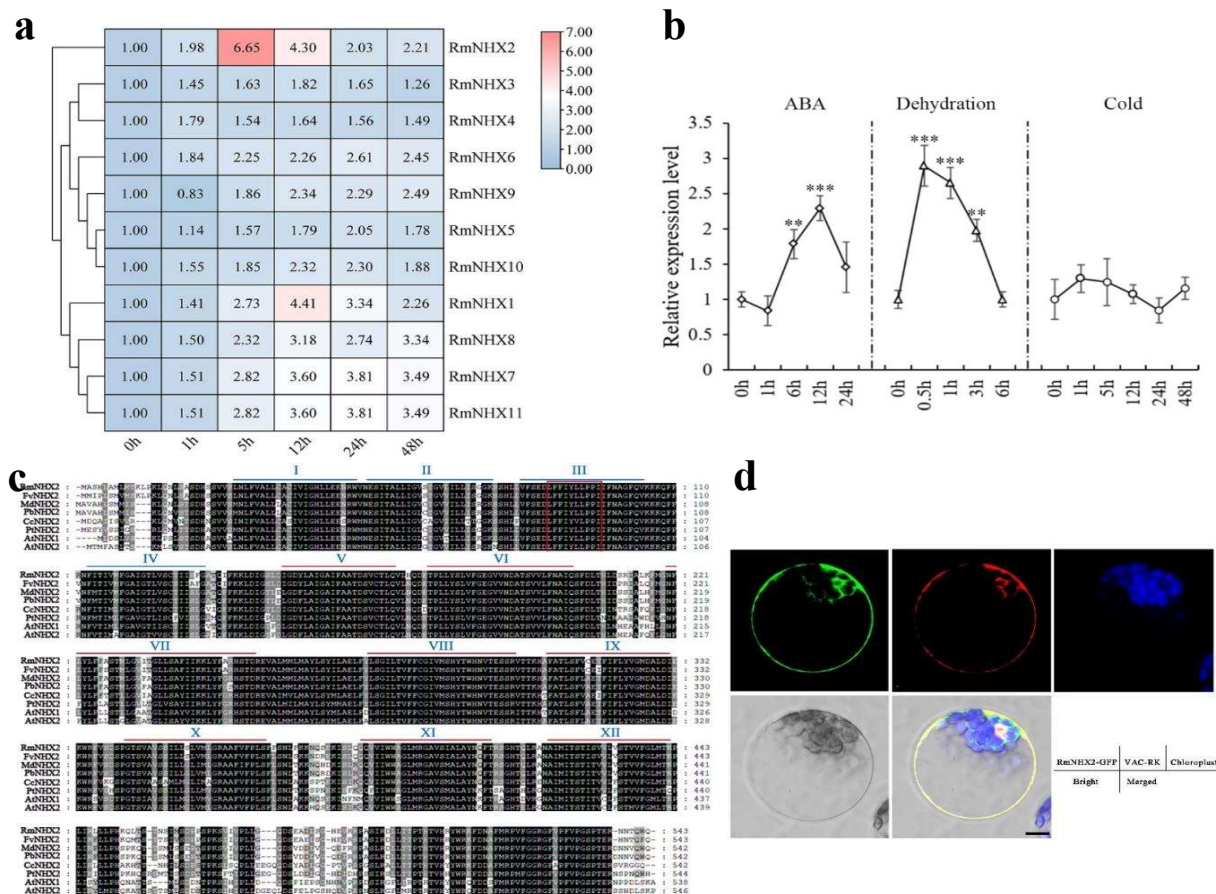


Figure 3. Time-course expression levels of *RmNHX* genes in *Rosa multiflora* under abiotic stress and subcellular localization analysis of *RmNHX2*. (a) Heatmap analysis of *RmNHX* genes in response to salt stress. (b) *RmNHX2* expression levels in *R. multiflora* exposed to cold, dehydration, and ABA. *RmGAPDH* was used as a reference gene. The expression level at timepoint 0 was defined as 1.0 and data represented means \pm SE of three replicates. Asterisks show values that are significantly different from that of the 0h (**, $p < 0.01$, ***, $p < 0.001$). (c) Amino acid sequence alignment of *RmNHX2* and other NHXs from other plants. Identical amino acids are shown with a black background and analogous amino acids are shaded in gray. The 12 typical transmembrane domains for a vacuolar-type Na^+/H^+ antiporter are shown by lines. The accession numbers of these known proteins in GenBank are: FvNHX2, XP_004289614.1; MdNHX2, XP_028954695.1; PbNHX2, XP_009352430.1; CcNHX2, XP_006433113.1; PtNHX2, XP_002307194.2; AtNHX1, NP_198067.1; and AtNHX2, NP_001326210.1. The different color stand for transmembrane domains. (d) Subcellular localization of *RmNHX2*. Arabidopsis protoplasts cells were transiently transformed with constructs containing fusion plasmid (*RmNHX2*: GFP) and tonoplast located marker (VAC: RK). Signals from GFP imaged using a laser scanning microscope. VAC: RK signals, merged images of GFP and RFP signals, and bright field. Bar = 10 μm . Three biological experiments were performed, which produced similar results.

The coding sequence of *RmNHX2* was 1632 bp, encoding a 543-amino-acids-containing protein. *RmNHX2* was deposited in GenBank with accession number MW358917. As revealed from multiple sequence alignment, *RmNHX2* shared 12 conserved transmembrane domains highly consistent with *FvNHX2* (94.11%) (Figure 3c). The amotif scanning suggested that the amiloride binding site (87-LFFIYLLPPI-96) existed in the N-terminal of *RmNHX2* (Figure 3c). A phylogenetic tree was constructed based on transmembrane domains of *RmNHX2* and 18 NHX proteins from other plant species (Figure 1A), in which *PtrERF109* was most closely related to *FvNHX2* (Figure S2). The structure and function of plant NHXs were closely related to their subcellular locations.

To determine the putative subcellular location of *RmNHX2*, its open reading frame (ORF) without a stop codon was inserted into the pHBT-GFP-NOS vector as driven by CaMV 35S, generating a fusion protein *RmNHX2*-GFP. In addition, the tonoplast marker protein VAC-RK was fused to C-terminal RFP. The mentioned plasmids were co-transformed into *Arabidopsis* protoplast cells. As demonstrated from transient expression assays, the green fluorescence of *RmNHX2*-GFP perfectly overlapped with tonoplast marker fluorescent signals (Figure 3d). The mentioned results suggested that *RmNHX2* was localized at the tonoplast.

2.3. *RmNHX2* Overexpression in Tobacco Led to Enhanced Salt Tolerance

As *RmNHX2* expression was strongly upregulated by salt, this study speculated that *RmNHX2* might perform important functions against salt stress. To test the role of *RmNHX2* in salt tolerance in depth, tobacco transgenic plants were generated through the leaf culture dish transformation. In total, twelve positive transgenic lines were identified using genomic PCR analysis (Figure S3). Additionally, three *RmNHX2* overexpressing (hereafter designated as OE1, OE7, and OE9, Figure S3) with higher expressing levels of *RmNHX2* were chosen for further experiment. To determine whether *RmNHX2* overexpression led to the increased salt stress resistance of the transgenic plants, the fully expanded leaves detached from 40-day-old *RmNHX2*-overexpressing lines and wild type tobacco (WTt) were administrated with 200 mM NaCl for 24 h. Before salt treatment, WTt and transgenic tobacco lines did not show any noticeable difference in morphology. However, the WTt leaves showed serious wilting as compared with the transgenic tobacco lines after incubation in 200 mM salt solution (Figure 4A). The electrolyte leakage (EL) and malondialdehyde (MDA) as vital indicators of cell damage were measured after salt stress between transgenic lines and WTt. The EL of the transgenic lines (25.7% for OE1, 34.5% for OE7, and 37.1% for OE9) were significantly lower than 52.7% of WTt (Figure 4B). According to Figure 4C, the MDA level was prominently lower in the transgenic lines than in WTt after the salt stress. In addition, we also determined the long-time salt stress tolerance of the potted plants. When 1-month-old plants were subjected to 200 mM NaCl for 14 d, the WTt exhibited a more serious wilting or necrosis compared with the *RmNHX2* overexpressing lines (Figure 4D). Consistent with the enhanced salt tolerance phenotype, the content of EL and MDA in the transgenic lines was significantly lower than in the WTt after salt stress (Figure 4E,F), indicating that cellular damage was more serious in the WTt. Furthermore, higher Chl level in transgenic lines compared with WTt was observed (Figure 4G). The mentioned results demonstrated that *RmNHX2* overexpression could increase the salt tolerance of transgenic tobacco.

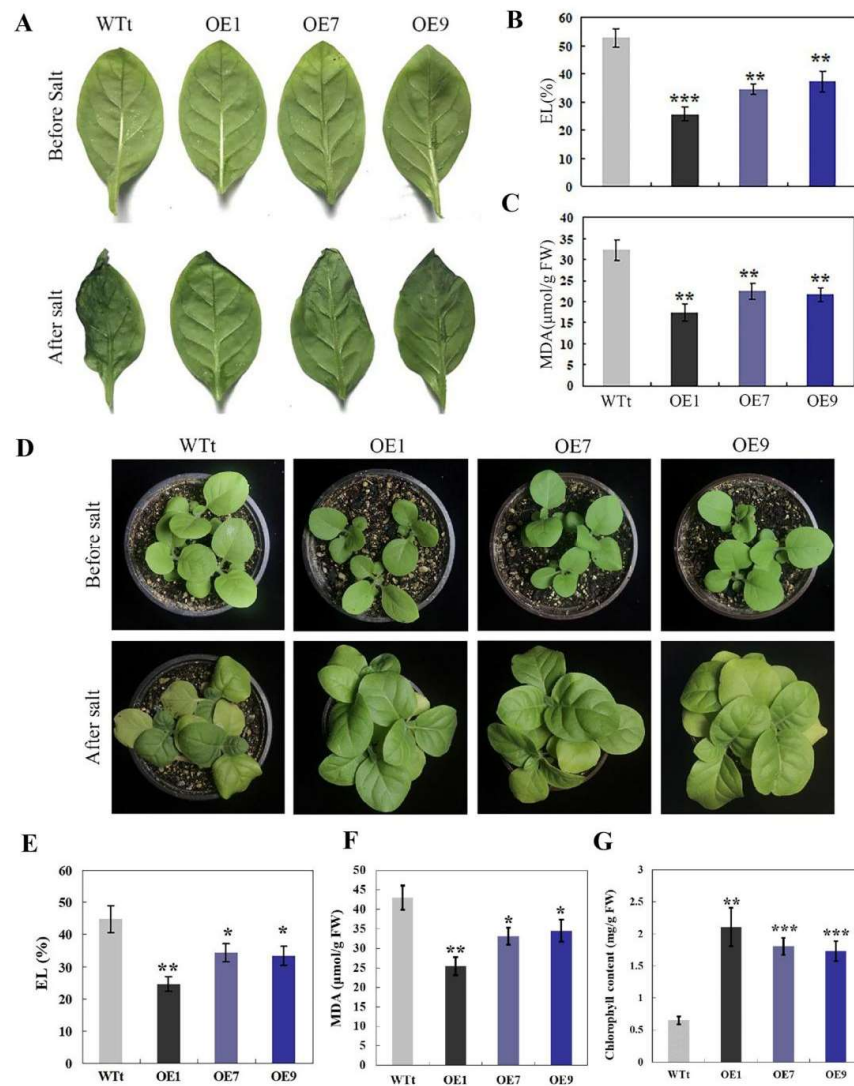


Figure 4. Overexpression of *RmNHX2* conferred enhanced salt tolerance in tobacco. (A) Leaf morphology of WTt and transgenic tobacco lines before and after treatment with 200 mM NaCl for 24 h. (B) Electrolyte leakage (EL) of the WTt, OE-1, OE-7, and OE-9 after 200 mM NaCl treatment for 24 h. (C) MDA levels of WTt, OE-1, OE-7, and OE-9 after 200 mM NaCl treatment for 24 h. (D) Phenotypes of 30-day-old plants of transgenic lines (OE-1, OE-7, and OE-9) and WTt before and after 200 mM NaCl treatment for 14 d. (E–G) Electrolyte leakage (E), MDA (F), and chlorophyll contents (G) of the WTt, OE-1, OE-7, and OE-9 after 200 mM NaCl treatment for 14 d. Error bars represent \pm SE ($n = 3$). Asterisks indicate significant differences between transgenic lines and WT ($* p < 0.05$, $** p < 0.01$, and $*** p < 0.001$).

2.4. Silencing of *RmNHX2* in *R. multiflora* Conferred Sensitivity to Salt Stress

To further elucidate the function of *RmNHX2* in salt tolerance, the VIGS system was conducted to silence *RmNHX2* expression in *R. multiflora*. The transcript level of *RmNHX2* in the VIGS plants was suppressed in comparison with that of the empty vector (pTRV2) transformed control plants (WTr) (Figure S4). We further assessed the salt tolerance of the mentioned two pTRV2-*RmNHX2* VIGS plants (designated as pTRV2-1 and pTRV2-2) exposed to salt stress. First, both the pTRV2-*RmNHX2* VIGS and WTr plants grown in hydroponic solution were exposed to 300 mM NaCl for 7 d. After the salt treatment, the VIGS lines showed more severe wilting phenotypes in comparison with the WTr (Figure 5A). In addition, EL and MDA, related to the cell damages, were determined. At the end of salt stress, the EL of pTRV2-1 (62.0%) and pTRV2-2 (59.0%) was significantly higher as

compared with 46.4% of WTr (Figure 5B). Meanwhile, the pTRV2-1 and pTRV2-2 presented higher MDA relative to WTr after the salt stress (Figure 5C). As shown in Figure 5D, the total chlorophyll content of the *RmNHX2*-VIGS plants were nearly 2-fold lower than that of WTr under salt stress.

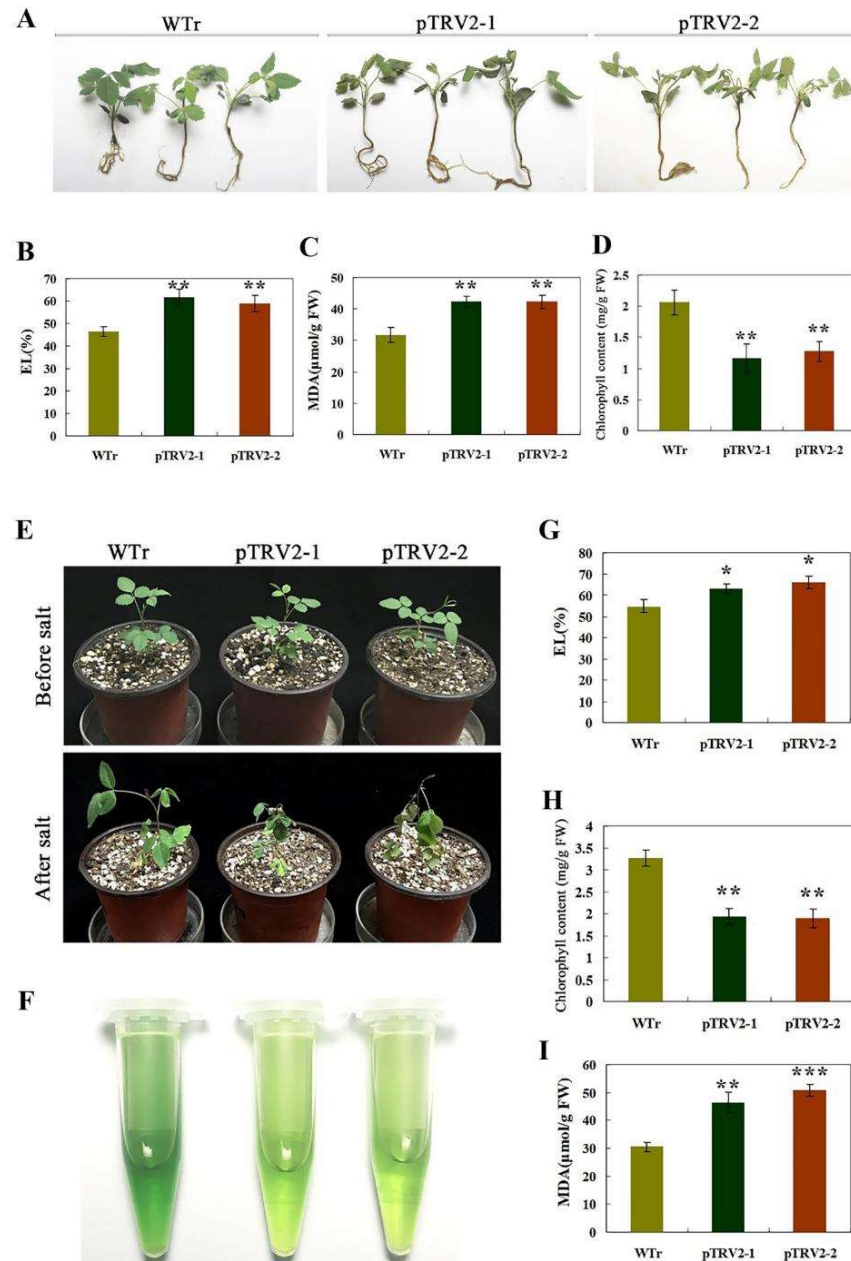


Figure 5. Silencing of *RmNHX2* led to enhanced salt sensitivity in *R. multiflora*. (A) Phenotypes of 15 d VIGS plants (pTRV2-1 and pTRV2-2 and wild rose (WTr) after salt treatment (300 mM NaCl for 7 d). (B–D) EL (B), MDA (C), and chlorophyll contents (D) of VIGS plants and WTr after the 7-d salt treatment. (E) Phenotypes of 30 d VIGS potted plants and wild rose (WTr) before and after salt treatment (300 mM NaCl for 14 d). (F) The chlorophyll extraction solutions of *RmNHX2* silenced plants at the end of salt stress. (G–I) EL (G), MDA (H), and chlorophyll contents (I) of VIGS plants and WTr after the 14 d 300 mM NaCl treatment. Error bars represent \pm SE (n = 3). Asterisks indicate significant differences between transgenic lines and WT (* $p < 0.05$, ** $p < 0.01$, and *** $p < 0.001$).

To gain insights into whether *RmNHX2* was associated with salt tolerance, the *RmNHX2*-VIGS plants and WTr were treated at 300 mM NaCl. No visible phenotypic differences were identified between the *RmNHX2*-VIGS plants and WTr without salt stress. After the salt treatment for 10 d, the pTRV2-1 and pTRV2-2 plants suggested more serious damage relative to the WTr plants (Figure 5E). When the salt treatment was completed, the chlorophyll extraction of WTr was displayed as a paler color than the *RmNHX2*-VIGS plants (Figure 5F). Consistent with the observed phenotype, the EL and MDA in the *RmNHX2*-VIGS plants were prominently higher than those of the WTr, implying that the VIGS plants were damaged to a greater degree (Figure 5G,H). Furthermore, the pTRV2-1 and pTRV2-2 plants achieved significantly lower levels of total chlorophyll than those of WTr after salt stress (Figure 5I). Regarded together, the mentioned data suggested that the silencing of *RmNHX2* in *R. multiflora* led to the elevated the salt sensitivity.

2.5. Analysis of H_2O_2 and O_2^- in Transgenic Tobacco and *R. multiflora* Silenced Plants under Salt Stress

Abiotic stresses were extensively evidenced to often induce ROS accumulation, thereby causing serious oxidative damage. ROS accumulation refers to a major indicator of stress tolerance. To verify whether *RmNHX2* is closely associated with the enhanced salt tolerance of plants, ROS scavenging, DAB, and NBT were performed to detect H_2O_2 and O_2^- productions, respectively, in transgenic and wild-type plants after the salt stress. Under 30-day-old tobaccos grown in soil pots administrated with 200 mM NaCl for 14 d, the WTt leaf discs were stained deeper and more intensely using nitro blue tetrazolium (NBT) and 3,3' diaminobenzidine (DAB) compared with the *RmNHX2*-overexpressing transgenic lines (Figure 6A,B). In contrast to the mentioned, deeper DAB and NBT staining were visualized in pTRV2-*RmNHX2* plants in contrast to the control plants (Figure 6C,D), implying that the ROS accumulation was enhanced when *RmNHX2* was silenced. For the verification of DAB and NBT staining results, the authors determined the H_2O_2 and O_2^- levels in the salt-treated leaves as well. Consistent with the staining, the levels of H_2O_2 and O_2^- were significantly lower in the transgenic tobacco lines compared with WTt, as indicated by the measured results (Figure 6E,F). In contrast, the pTRV2-*RmNHX2* VIGS plants accumulated more ROS than the WTr did (Figure 6G,H). Both results suggested that the *RmNHX2* overexpression led to the lower ROS accumulation in comparison with the WTt after salt treatment, whereas they also showed the opposite when *RmNHX2* was downregulated.

2.6. Analysis of Antioxidant Enzyme Activities and Expression Levels of the Encoding Genes in Transgenic Tobacco and *R. multiflora* Silenced Plants under Salt Stress

As antioxidant enzymes are involved in the regulation of ROS scavenging, we analyzed the catalase (CAT), peroxidase (POD), and superoxide dismutase (SOD) enzyme activities. When the 30-day-old potted tobacco plants were exposed to the salt treatment for 14 d, the activities of the CAT, POD, and SOD in the transgenic plants were significantly higher than those in the WTt (Figure 7A–C). Furthermore, the expression levels of CAT, POD, and SOD in *RmNHX2* overexpression tobacco plants were significantly upregulated compared with that in the WTt after salt treatment (Figure 7D–F). In contrast to the mentioned, three noticeably lower enzyme activities were observed in the two VIGS plants (pTRV2-1 and pTRV2-2) than in the WTr plants at the end of salt stress (Figure 7G–I). However, it was displayed the opposite way when the *RmNHX2* expression was downregulated (Figure 7J–L). The mentioned finding suggested that *RmNHX2* functioned in salt tolerance, at least partially, resulting from the increased actions of CAT, POD, and SOD.

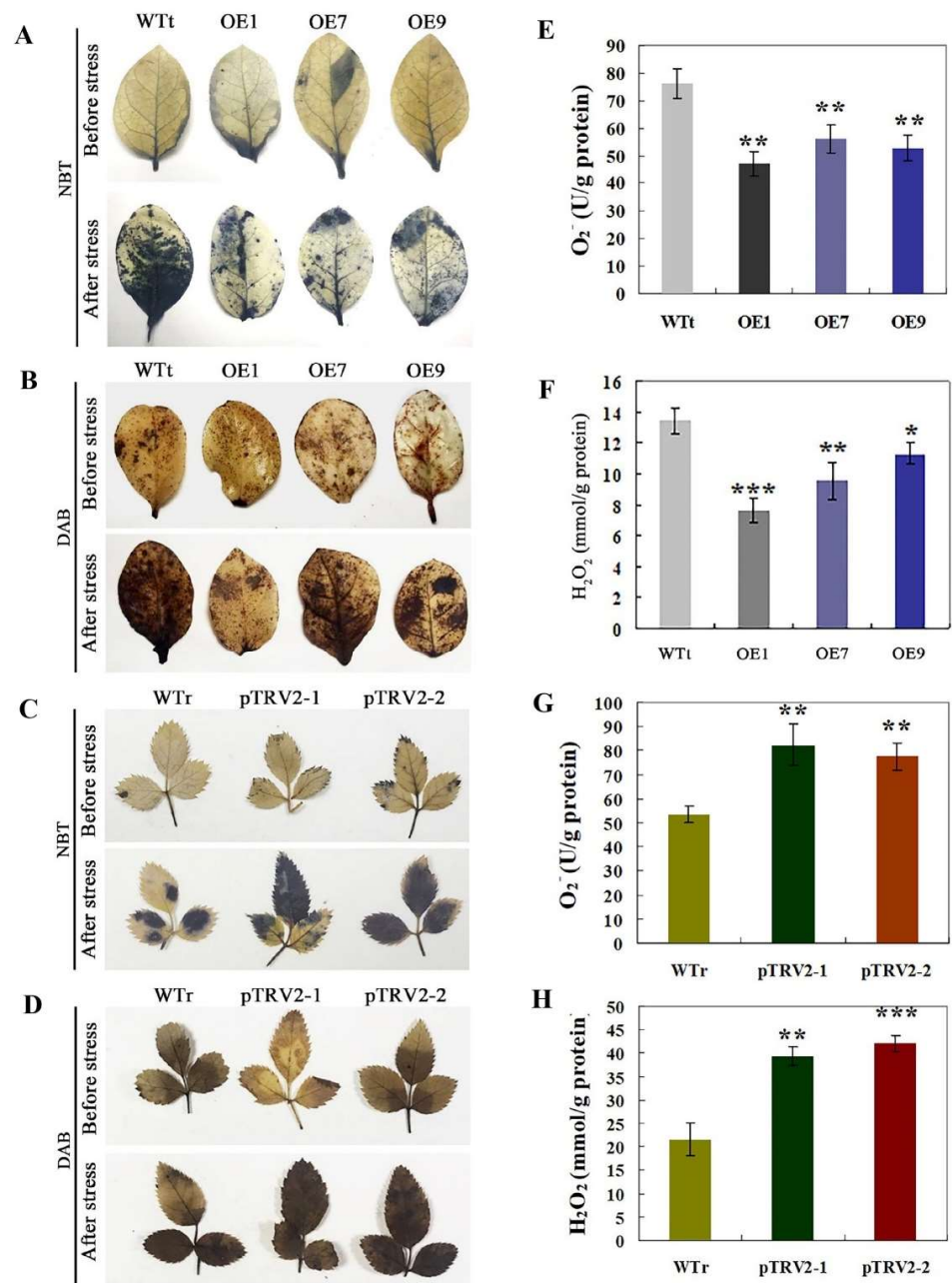


Figure 6. Analysis of O_2^- and H_2O_2 in transgenic tobacco and *R. multiflora* silenced plants after salt stresses. (A) Histochemical staining using NBT for detection of O_2^- in WTt, OE-1, OE-7, and OE-9 before and after 14 d of 200 mM NaCl. (B) Histochemical staining with DAB for detection of H_2O_2 in WTt, OE-1, OE-7, and OE-9 before and after 14 d of 200 mM NaCl. (C) Representative photos showing accumulation of O_2^- in WTr and wild rose silenced plants before and after 14 d of 300 mM NaCl. (D) Representative photos showing accumulation of H_2O_2 in WTr and wild rose silenced plants before and after 14 d of 300 mM NaCl. (E,F) Levels of O_2^- (E) and H_2O_2 (F) in tobacco WTt and transgenic lines (OE-1, OE-7, and OE-9) after 14 d of 200 mM NaCl stress. (G,H) Levels of O_2^- (G) and H_2O_2 (H) in wild rose WTr and silenced plants (pTRV2-1 and pTRV2-2) after 14 d of 300 mM NaCl stress. Error bars represent \pm SE ($n = 3$). Asterisks indicate significant differences between transgenic lines and WT (* $p < 0.05$, ** $p < 0.01$, and *** $p < 0.001$).

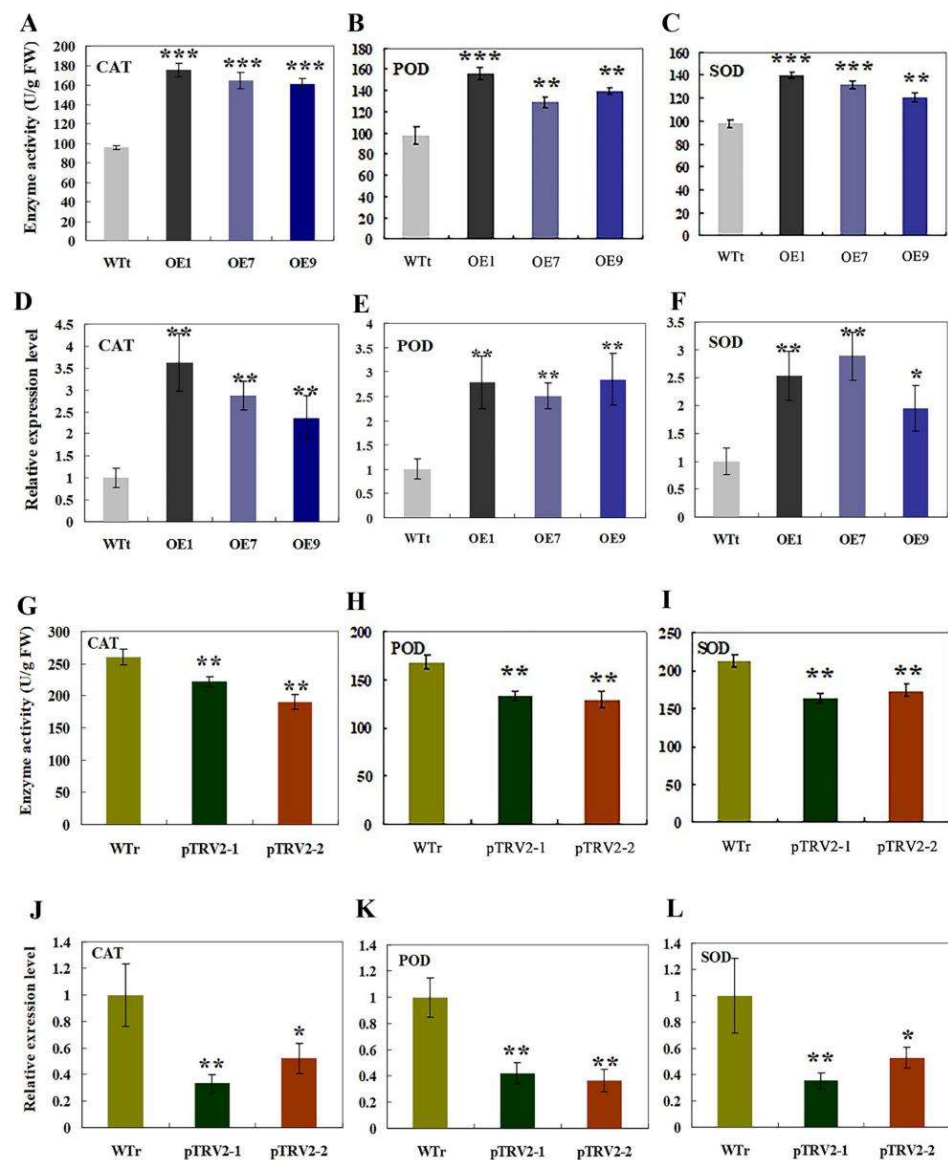


Figure 7. Analysis of enzyme activities and gene expression levels related to antioxidant enzymes in tobacco and *Rosa multiflora* pTRV-*RmNHX2* silenced plants after salt stress. (A–C) The activities of CAT (A), POD (B), and SOD (C) in the WTt and transgenic tobacco plants after 14 d of 200 mM NaCl treatment. (D–F) The expression level of CAT (D), POD (E), and SOD (F) in the WTt and transgenic tobacco plants after 14 d of 200 mM NaCl treatment. (G–I) The activities of CAT (G), POD (H), and SOD (I) in the WTr and *Rosa multiflora* pTRV-*RmNHX2* silenced plants after 14 d of 300 mM NaCl treatment. (J–L) The expression of CAT (J), POD (K), and SOD (L) in the WTr and *Rosa multiflora* pTRV2-*RmNHX2* silenced plants after 14 d of 300 mM NaCl treatment. Error bars represent \pm SE (n = 3). Asterisks indicate significant differences between transgenic lines and WT (* $p < 0.05$, ** $p < 0.01$, and *** $p < 0.001$).

2.7. Opposite Accumulation of Na^+ and K^+ in Transgenic Tobacco and *Rosa multiflora* Silenced Plants under Salt Stress

A plant's Na^+ balance is disrupted under salt stress. As ionic homeostasis is a major factor causing salt stress, we therefore examined the accumulation of Na^+ and K^+ in the leaves and roots. Upon exposure to salt stress, the Na^+ levels were 11.91 mg/g dry weight (DW) in WTt tobacco roots, 7.38 mg/g DW in OE1, 8.76 mg/g DW in OE7, and 9.63 mg/g DW in OE9 (Figure 8A). The Na^+ levels of leaves were lower in the OE1, OE7, and OE9 as compared with those in the WTt (Figure 8A). Moreover, the leaves and roots in the

RmNHX2 overexpression tobacco plants accumulated more K^+ than those in the WTt leaves and roots (Figure 8B). As a result, the Na/K ratios in WTt were noticeably higher than in the transgenic tobacco lines after salt treatment (Figure 8C). Conversely, the levels of Na^+ , K^+ , and Na/K in the two pTRV2-*RmNHX2* VIGS lines were significantly higher or lower than those of the WTr plants after salt stress, respectively (Figure 8D–F). The mentioned data demonstrated that the enhanced tolerance of transgenic tobacco lines and susceptibility of pTRV2-*RmNHX2* VIGS plants to salt stress were closely related to ion homeostasis.

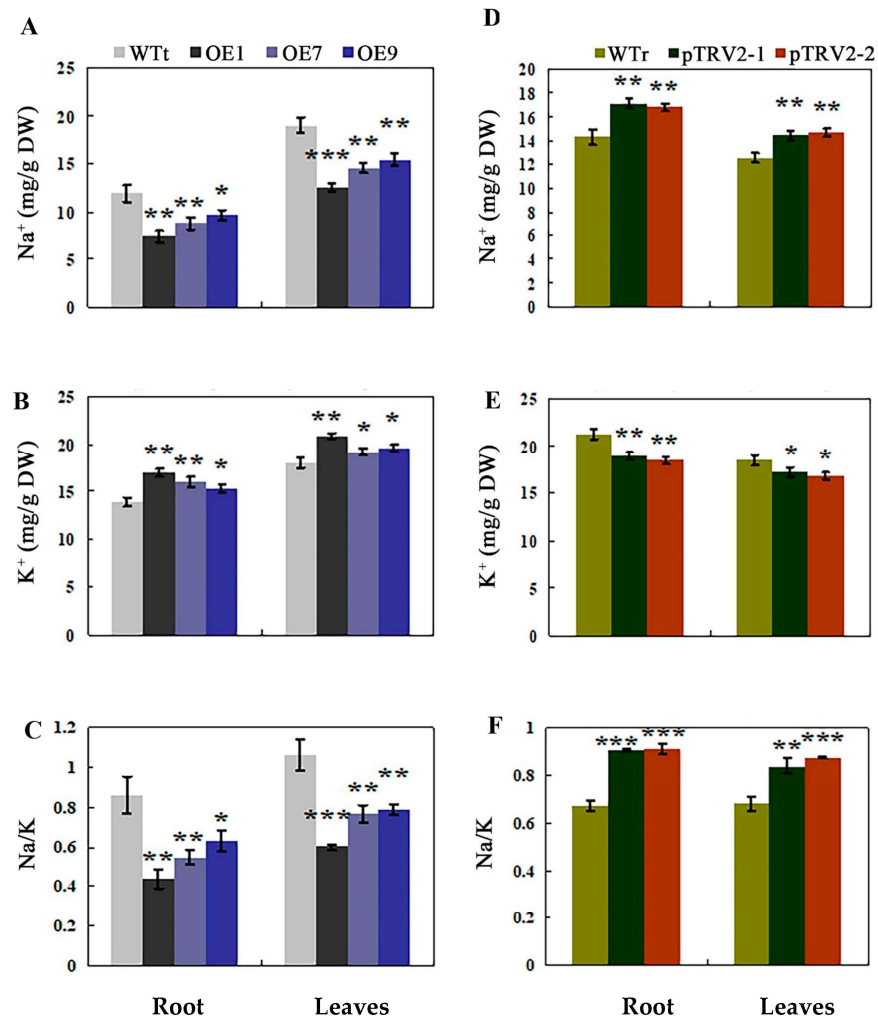


Figure 8. Ion levels in the leaves and roots of tobacco and *Rosa multiflora* pTRV2-*RmNHX2* silenced plants after salt stress. (A–C) The contents of Na^+ (A), K^+ (B), and the Na/K ratio (C) in the WTt and transgenic tobacco plants after 14 d of 200 mM NaCl treatment. (D–F) The contents of Na^+ (D), K^+ (E), and the Na/K ratio (F) in the WTr and *Rosa multiflora* pTRV2-*RmNHX2* silenced plants after 14 d of 300 mM NaCl treatment. Error bars represent \pm SE (n = 3). Asterisks indicate significant differences between transgenic lines and WT (* $p < 0.05$, ** $p < 0.01$, and *** $p < 0.001$).

3. Discussion

Previous studies have shown that plant intracellular Na^+/H^+ antiporters play significant roles in adaption to salt stress through the maintenance of the cellular PH and ionic equilibrium [18,19]. Though several NHXs have been described in the model plants, e.g., *Arabidopsis thaliana*, rice, and cotton, knowledge is still limited concerning the function and action mechanism of plant NHXs in perennial woody ornamental plants. Thus, clarifying NHXs function in perennial plants, e.g., *Rosa multiflora*, will provide a better understanding on the role of NHXs.

In this study, we confirmed 11 *RmNHXs* in *Rosa multiflora* through the genome-wide analysis. *RmNHXs* showed alteration of transcript levels in response to salt stress, of which *RmNHX2* was particularly elevated. As revealed from the multiple sequences alignment of *RmNHX2* and other plants *NHXs*, *RmNHX2* contained twelve transmembrane domains and amiloride binding motif in the N-terminal. Thus, *RmNHX2* could be clustered into the typical *NHX* group. The phylogenetic analysis indicated that *RmNHX2* pertained to the vacuolar Na^+/H^+ antiporter proteins and displayed closer associations with FvH4 (6g04140.1).

A number of studies had presented data suggesting that one of the main features of plants *NHXs* was the upregulation of their transcript level by salt stress [20,21]. In this study, *RmNHX2* was induced to the greatest degree by salt treatment, implying that *RmNHX2* may play a critical role in the regulation of the salt response. To verify this assumption, transgenic tobacco lines overexpressing *RmNHX2* were obtained. As for expectation, *RmNHX2* overexpression also enhanced the salt tolerance in tobacco, as revealed by lower MDA and EL contents than the WTt, which was consistent with previous reports [22,23]. MDA and EL are two key indicators of lipid peroxidation, displaying a close relationship to the membrane systems [24]. Thus, it is normally proposed that the *RmNHX2* overexpression lines experienced a lower degree of membrane injuries in comparison with WTt when exposed to salt stress. On the whole, environmental stress led to the excessive accumulation of ROS as well (e.g., H_2O_2 and O_2^-), thereby probably inducing the lipid peroxidation. Thus, the ROS forming and concentration pattern were usually used as a key indicator to evaluate the stress tolerance [25]. Of special note, the transgenic tobacco lines accumulated significantly less H_2O_2 and O_2^- than WTt using DAB and NBT staining, suggesting that transgenic plants suffered from milder salt stresses, which agreed with the measured data of MDA and EL. This provides convincing evidence to show that the *RmNHX2* functions in salt tolerance, at least partially, because of the lower concentration of ROS.

This is further supported by concurrent observation of an elevation of ROS contents and increased salt sensibility in the VIGS lines with the silencing of *RmNHX2*. ROS accumulation under stress condition displays a tight association with the equilibrium between ROS accumulation and scavenging [26]. The ROS-scavenging enzymes (e.g., SOD, CAT, and POD) positively impacted ROS detoxification to alleviate cell damage under environmental stresses [27]. In subsequent experiments, the SOD, POD, and CAT activities noticeably increased in transgenic lines as compared with those of the WTt under the salt stress. The greater enzyme activities may account for the accumulation of less ROS in the mentioned lines. However, the expression levels of antioxidant genes were significantly downregulated in the *RmNHX2*-VIGS lines, which complied with the higher contents of ROS. Increasing evidence demonstrated that a high antioxidant capacity to scavenge the ROS is linked to increased tolerance to environmental stresses [25]. This study demonstrated that *RmNHX2* (a vacuolar Na^+/H^+ antiporter) regulate the Na^+ and K^+ homeostasis, which promoted optimal conditions in cytosol and organelles to function as antioxidative enzymes.

It is conceivable that excessive cytosolic Na^+ accumulation in plant cells induced cell injury and ionic toxicity as well, thereby resulting in ion imbalance and a perturbation of the Na:K ratio [28,29]. The membrane potential and the activity of many essential enzymes were also disturbed by the excessive Na^+ , which led to osmotic imbalance [30]. In addition, the level of K^+ in cellular also affects the salt tolerance of plants [31]. The uptake of K^+ was also inhibited by external Na^+ , resulting in K^+ deficiency in the cytosol and an increase in the Na/K ratio. In the present study, the *RmNHX2* overexpression tobacco lines showed the enhanced tolerance of salt with a lower Na^+ level but with higher concentrations of K^+ and reduced Na/K ratios, whereas the salt sensitivity of the *RmNHX2* VIGS lines was consistent with the higher Na^+ level, reduced K^+ , and increased Na/K ratio. Thus, the enhanced salt tolerance of *RmNHX2* overexpression tobacco lines might be ascribed to the efficient maintenance of the ion balance.

4. Materials and Methods

4.1. Identification of the NHX Family Genes in *Rosa multiflora*

The annotated protein sequences of *Rosa multiflora* were downloaded from the *R. multiflora* Genome database (<http://kazusa.or.jp/index.html>) (accessed on 2 May 2022). The Hidden Markov Model (HMM) file corresponding to the Na⁺/H⁺ exchanger domain (PF00999) was downloaded from the Pfam protein family database (<http://pfam.xfam.org/>) (accessed on 11 May 2022). TBtools was employed to obtain the putative RmNHXs in *Rosa multiflora* (E-value < 1 × 10⁵) [32]. The existence of the conserved Na⁺/H⁺ exchanger domain was examined using the SMART (<http://smart.emblheidelberg.de/>) (accessed on 13 May 2022) and NCBI-CDD search (<http://www.ncbi.nlm.nih.gov/Structure/cdd/wrpsb.cgi>) (accessed on 13 May 2022). The sequences without the Na⁺/H⁺ exchanger domain were excluded. The online program ExPasy (http://web.expasy.org/compute_pi/) (accessed on 13 May 2022) was used to predict the molecular weight (Mw) and isoelectric point (pI) of the putative RmNHXs. According to the conserved domains of NHXs in wild rose, rosa, strawberry, apple, cherry, raspberry, and *Arabidopsis*, a phylogenetic tree was constructed in MEGA7.0 (Kumar, Philadelphia, USA) using the Neighbor-Joining (NJ) method (bootstrap = 1000).

4.2. Gene Structure, Conserved Motif and Promoter Analyses

Gene Structure Display Server (<http://gsds.cbi.pku.edu.cn/>) (accessed on 15 May 2022) was employed for intron and exon analysis. The conserved motifs in the protein sequences were examined using Pfam. The cis-acting elements in the promoters (up to 2000-bp upstream ATG) of the *RmNHXs* genes were analyzed using PlantCARE (<http://bioinformatics.psb.ugent.be/webtools/plantcare/html>) (accessed on 23 May 2022).

4.3. Plant Material and Stress Treatment

The seeds of *Rosa multiflora* were collected in the Zhejiang A&F University Rose Germplasm Resources. The seeds stored in humid sand were maintained at the temperature of 4 °C. After 2 months, the seeds were transferred into plugs in an artificial climate box of 16 h light/8 h dark cycles at 22 °C. The 60-day-old *Rosa multiflora* seedlings underwent exposure to stress treatment to analyze the *RmNHXs* expression pattern. For the salt treatment, each seedling was sprayed with 50 mL of 200 mM NaCl solution and sampled after 1, 5, 12, 24, and 48 h in a growing chamber. At least 40 uniform seedlings were employed for salt stress treatment. The leaves were harvested from 4 seedlings harvested in a random manner under the set points of the respective treating processes and blended as a pool of sample materials. The leaf samples were promptly frozen in liquid nitrogen and then stored in −80 °C until their utilization.

4.4. RNA Extracting Process and Quantitative Real-Time PCR Study (qRT-PCR)

By using an Easyspin Plant RNA Kit (Aidlab, Beijing, China) following the instructions for use, the total RNA was extracted from the samples. Subsequently, 1 µg of total RNA was reversely transcribed to cDNA by using PrimeScript RT Reagent Kit With gDNA Eraser (TaKaRa, Dalian, China). Based on a 7500 real-time PCR cycler (Applied Biosystems, Waltham, MA, USA) and the SYBR Premix Ex Based on (TaKaRa, Dalian, China), qRT-PCR was performed. Table S2 lists the sequences of primers. This study determined the relative expression level of target genes by using the 2^{−ΔΔCt} method [33]. For *Rosa multiflora*, *RmGAPDH* was used as the internal control and *NtEF1* was used as reference gene in tobacco. The expression level of each time point was detected at least three times, and the data are expressed as the mean values ± SE.

4.5. Isolation of *RmNHX2* and Sequence Analysis

The *RmNHX2* coding sequence was amplified using high-fidelity Ex Taq (TaKaRa, Dalian, China) with gene-specific primers (Table S2); next, the ligation into pMD 18-T vector (TaKaRa, Dalian, China) was conducted. It was confirmed by sequencing (TsingKe,

Hangzhou, China). Based on ClustalW, several sequence alignments were conducted and presented using GeneDoc Software (K.B. Nicholas, San Francisco, CA, USA).

4.6. Subcellular Localizing Process of *RmNHX2*

To achieve the subcellular localization, the *RmNHX2* coding sequence without the stop codon was amplified by using specific primers (Table S2), and it was then cloned into the pHBT-GFP-NOS vector at the *Bam*HI and *Sal*I restriction sites as promoted by the CaMV 35S. The isolation of the *Arabidopsis* protoplasts was conducted in line with the existing studies [34]. Next, 10 µg of *RmNHX2*-GFP plasmid was gently mixed with 100 µL of the *Arabidopsis* protoplasts (105/mL) and the mixture was incubated at 23 °C for 12 h. Under a laser scanning microscope (LSM410, Carl Zeiss, Oberkochen, Germany), the green and red fluorescence signals in *Arabidopsis* protoplasts were detected.

4.7. Generation of *RmNHX2*-Overexpressing Tobacco Lines

The CDS region of *RmNHX2* was amplified from pMD 18-T-*RmNHX2* by using specific primers (Table S2) that contained *Bam*HI and *Sal*I restriction sites and ligated into the identical sites of the expression vector pCambia2300s, which was controlled by the CaMV 35S. Based on the freeze–thaw method, the resulting plasmid was transformed to *A. tumefaciens* strain (EHA105). Tobacco (*Nicotiana tabacum* cv. 'Xianzi') genetic transformation was conducted by complying with the existing study [35]. The transgenic tobacco lines were placed in a growth chamber (25 °C, 16 h light/8 h dark). Besides, the molecular identification of the regenerated plants was confirmed based on PCR by using two pairs of specific primers (Table S2). By RT-PCR, this study determined the *RmNHX2* expression levels in the positive transgenic tobacco lines were determined. To perform the subsequent experiments, the T2 seeds of transgenic tobacco lines were adopted.

4.8. Generation of *RmNHX2* Silenced Plants by Virus-Induced Gene Silencing (VIGS)

Following the previous study [25], virus-induced gene silencing (VIGS)-mediated suppression of *RmNHX2* was conducted. Here, based on PCR with specific primers, the *RmNHX2* ORF (52–531 bp)'s 487 bp fragment was obtained from a pMD 18-T-*RmNHX2* vector (Table S2). The PCR product was inserted into *Xba* I and *Sac* I locations of pTRV2 to produce pTRV2-*RmNHX2*. The pTRV1, pTRV2, and pTRV2-*RmNHX2* vectors were added to *A. tumefaciens* strain (GV3101) using the freeze–thaw method. The VIGS-mediated suppression of *RmNHX* in *Rosa multiflora* was performed as described with minor modification [36]. The bacterial cells (OD₆₀₀ = 1.0) supplemented by pTRV1 were mixed with pTRV2-*RmNHX2* or pTRV2 at 1:1 (v/v) in an infiltration buffer (10 mM MgCl₂, 150 mM acetosyringone, 10 mM MES, and pH 5.6) and maintained under darkness for 3 h under ambient temperature. *Rosa multiflora* seeds with emerging shoots (c. 1 cm long) were immersed into the bacterial mixtures and infiltration was conducted under vacuum at –25 kPa twice, maintaining for 60 s. When the vacuum was released, the seeds were cleaned with distilled water and then planted in pots. The plants were grown in a growing chamber at 16 h light/8 h dark cycles at 22 °C, 70% relative humidity. After 10 d, the gene silencing efficiency was determined using qRT-PCR.

4.9. Salt Stress Tolerance Assay

A series of experiments were designed to elucidate the function of *RmNHX2* in response to the salt stress. First, the leaves detached from 40 d transgenic and WT tobacco (WTt) plants were exposed to 200 mM NaCl for 24 h. Electrolyte leakage (EL) and malondialdehyde (MDA) contents of the treated leaves were measured at the end of stress treatment. Second, 30 d potted *RmNHX2* overexpressing lines and control tobacco plants (WTt) were sprayed with 200 mM NaCl at 3 d intervals for 2 weeks. Moreover, 15 d *RmNHX2* silenced (VIGS) and *R. multiflora* (WTr) plantlets were hydroponically grown for 7 d in 300 mM NaCl solution. In another experiment, the *R. multiflora* 30 d VIGS potted plants were sprayed with 200 mL of 300 mM NaCl at 3 d intervals for 2 weeks. The respective treatment was

repeated three times with consistent results. The physiological, biochemical, and gene expression were performed after salt stress.

4.10. Physiological Analyses

The EL was determined as previously described [37]. Besides, the MDA, H_2O_2 , O_2^- contents, and antioxidant enzymes activities (i.e., CAT (EC 1.11.1.6), SOD (EC 1.15.1.1), and POD (EC 1.11.1.7) were also assayed with specific detection kits (Nanjing Jiancheng Bioengineering Institute, Nanjing, China) by complying with the manufacturer's protocol. Furthermore, the total chlorophyll in the leaves was extracted and determined according to the previous study [38]. The Na^+ and K^+ levels were determined under atomic absorption spectrophotometry using a previously described method [39]. In brief, the dry samples of leaves and roots were ground into powder. Approximately, 0.1 g of tissue powder was dissolved with 5 mL deionized distilled water, followed by boiling in water bath for 2 h. Lastly, the extract was filtered; then, the Na^+ and K^+ of the samples were measured.

4.11. In Situ Histochemical Staining of ROS

The H_2O_2 and O_2^- accumulations in the samples were stained using 3,3' diaminobenzidine (DAB) (CAS: 91-95-2) and nitro blue tetrazolium (NBT) (CAS: 298-83-9), respectively [40]. In summary, the leaves were immersed in 1 mg ml^{-1} DAB (in 50 mM potassium phosphate, pH 3.8) fresh solution or NBT (in 50 mM potassium phosphate, pH 7.8) for 12 h in the dark at ambient temperature. The above stained leaves were immersed in 100% ethanol until the chlorophyll faded and were subsequently maintained in 70% ethanol until being photographed.

4.12. Statistical Analysis

The salt treatment was repeated at least two times with the achieved consistent results. The representative one was presented, shown as mean \pm SE. The ANOVA was used to compare the statistical difference based on Fisher's least significant difference test; the statistical differences were determined at the significance level of $p < 0.05$ (*), $p < 0.01$ (**), and $p < 0.001$ (***)).

5. Conclusions

In this study, we confirmed 11 *RmNHX*s proteins in *Rosa multiflora* through the genome-wide analysis. *RmNHX2* was drastically and progressively elevated by the salt stress. *RmNHX2* was localized at the tonoplast. *RmNHX2* overexpression in tobacco led to the enhanced salt tolerance, while the downregulation of *RmNHX2* in *Rosa multiflora* increased salt susceptibility. The endogenous Na^+ concentration in the transgenic tobacco lines was reduced in the leaves and roots, leading to the lowered Na/K ratios. The *RmNHX2*-mediated salt tolerance might at least be in part via the antioxidant system and ion homeostasis (Figure 9). Accordingly, *RmNHX2*, as an important candidate gene, had a great potential for the molecular breeding of salt-tolerant woody ornamental plants.

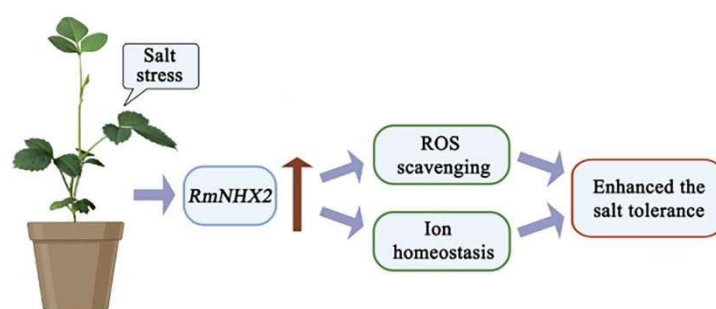


Figure 9. A proposed model of action for explaining regulatory function of *RmNHX2* in response to salt stress. Salt stress could upregulate the expression of *RmNHX2* in *Rosa multiflora*. *RmNHX2* enhances the salt tolerance via modulating the ROS scavenging system and ion homeostasis.

Supplementary Materials: The following supporting information can be downloaded at: <https://www.mdpi.com/article/10.3390/horticulturae9030290/s1>, Figure S1: Predicted cis-acting elements in *RmNHXs* promoters. The cis-acting elements are indicated in different colored boxes, Figure S2: Phylogenetic tree of *RmNHX2* protein with its homologous proteins from other plant species. MEGA 7 was used to construct the phylogenetic tree with the NJ method, Figure S3: Generation and molecular identification of transgenic tobacco plants overexpressing *RmNHX2*. (A) Schematic diagram of the *RmNHX2* overexpression construct used for tobacco transformation. 35S, cauliflower mosaic virus 35S promoter. (B–F) Transformation of *RmNHX2* into tobacco. (G) PCR confirmation of the kanamycin-resistant plants using CaMV35S- *RmNHX2* primers. M, molecular marker; +, plasmid DNA (used as a positive control); -, wild type; the numbers indicate different transgenic lines (lines 1, 7, and 9 are designated as OE1, OE7, and OE9, respectively). (H) Expression analysis of *RmNHX2* in three transgenic lines using RT-PCR. *NtEF1 α* gene was used as an internal control. Figure S4: Analysis of the transcript levels of *RmNHX2* in *Rosa multiflora* silenced plants and wild type (WTr). (A) Expression analysis of *RmNHX2* in two VIGS lines using RT-PCR. *RmGAPDH* gene was used as an internal control. (B) qRT-PCR analysis of *RmNHX2* in two VIGS lines. *RmGAPDH* gene was used as an internal control. Table S1: Summary of *RmNHXs* genes in *Rosa multiflora*. Table S2: Primer sequences used in this study.

Author Contributions: P.L. and Y.C. conceived the study and participated in its design. H.L., L.C. and Y.S. performed experiments. P.L. analyzed the data and wrote the manuscript. All authors have read and agreed to the published version of the manuscript.

Funding: This work was supported by grants from the National Natural Science Foundation of China (No. 31800598 and No. 32102419), the Natural Science Foundation of Zhejiang Province (No. LQ18C15000), and the Fundamental Research Funds for the Zhejiang A&F University (No. 2016FR033). The funders had no role in study design, data collection and analysis, decision to publish, or preparation of the manuscript.

Institutional Review Board Statement: Not applicable.

Informed Consent Statement: Not applicable.

Data Availability Statement: All data supporting the findings of this study are available from the corresponding author on reasonable request.

Acknowledgments: We thank Yin Bao for providing the tobacco seeds.

Conflicts of Interest: The authors declare no conflict of interest.

References

1. Mahajan, S.; Tuteja, N. Cold, salinity and drought stresses: An overview. *Arch. Biochem. Biophys.* **2005**, *444*, 139–158. [[CrossRef](#)]
2. Zhu, J.K. Salt and drought stress signal transduction in plants. *Annu. Rev. Plant Biol.* **2002**, *53*, 247–273. [[CrossRef](#)]
3. Kronzucker, H.J.; Britto, D.T. Sodium transport in plants: A critical review. *New Phytol.* **2011**, *189*, 54–81. [[CrossRef](#)]
4. Yoshida, T.; Mogami, J.; Yamaguchi-Shinozaki, K. ABA-dependent and ABA-independent signaling in response to osmotic stress in plants. *Curr. Opin. Plant Biol.* **2014**, *21*, 133–139. [[CrossRef](#)]
5. Giraud, E.; Aken, O.V.; Ho, L.H.M.; Whelan, J. The transcription factor ABI4 is a regulator of mitochondrial retrograde expression of *Alternative oxidase*. *Plant Physiol.* **2009**, *150*, 1286–1296. [[CrossRef](#)]
6. Zhang, X.M.; Cheng, Z.H.; Zhao, K.; Yao, W.J.; Sun, X.M.; Jiang, T.B.; Zhou, B. Functional characterization of poplar *NAC13* gene in salt tolerance. *Plant Sci.* **2019**, *281*, 1–8. [[CrossRef](#)]
7. Phukan, U.J.; Jeena, G.S.; Tripathi, V.; Shukla, R.K. MaRAP2-4, a waterlogging-responsive ERF from *Mentha*, regulates bidirectional sugar transporter AtSWEET10 to modulate stress response in *Arabidopsis*. *Plant Biotechnol. J.* **2017**, *16*, 221–233. [[CrossRef](#)]
8. Yu, J.L.; Ge, H.M.; Wang, X.K.; Tang, R.J.; Wang, Y.; Zhao, F.G.; Lan, W.; Luan, S.; Yang, L. Overexpression of pyrabactin resistance-like abscisic acid receptors enhances drought, osmotic, and cold tolerance in transgenic poplars. *Front. Plant Sci.* **2017**, *8*, 1752. [[CrossRef](#)]
9. Dong, W.; Wang, M.C.; Xu, F.; Quan, T.Y.; Peng, K.Q.; Xiao, L.T.; Xia, G. Wheat oxophytodienoate reductase gene *TaOPR1* confers salinity tolerance via enhancement of abscisic acid signaling and reactive oxygen species scavenging. *Plant Physiol.* **2013**, *161*, 1217–1228. [[CrossRef](#)]
10. Shelake, R.M.; Kadam, U.S.; Kumar, R.; Pramanik, D.; Singh, A.K.; Kim, J.Y. Engineering drought and salinity tolerance traits in crops through CRISPR-mediated genome editing: Targets, tools, challenges, and perspectives. *Plant Commun.* **2022**, *6*, 208–234. [[CrossRef](#)]

11. Banjara, M.; Zhu, L.F.; Shen, G.X.; Payt, P.; Zhang, H. Expression of an *Arabidopsis* sodium/proton antiporter gene (*AtNHX1*) in peanut to improve salt tolerance. *Plant Biotechnol. Rep.* **2012**, *6*, 59–67. [[CrossRef](#)]
12. Yuan, H.J.; Ma, Q.; Wu, G.Q.; Pei, W.; Jing, H.; Wang, S.M. *ZxNHX* controls Na⁺ and K⁺ homeostasis at the whole-plant level in *Zygophyllum xanthoxylum* through feedback regulation of the expression of genes involved in their transport. *Ann. Bot.* **2015**, *115*, 495–507. [[CrossRef](#)]
13. Deinlein, U.; Stephan, A.B.; Horie, T.; Luo, W.; Schroeder, J.I. Plant salt-tolerance mechanisms. *Trends Plant Sci.* **2014**, *19*, 371–379. [[CrossRef](#)]
14. Bassil, E.; Blumwald, E. The ins and outs of intracellular ion homeostasis: NHX type cation/H⁺ transporters. *Curr. Opin. Plant Biol.* **2014**, *22*, 1–6. [[CrossRef](#)]
15. Bassil, E.; Tajima, H.; Liang, Y.; Ohto, M.; Ushijima, K.; Nakano, R.; Esumi, T.; Coku, A.; Belmonte, M.; Blumwald, E. The *Arabidopsis* Na⁺/H⁺ antiporters NHX1 and NHX2 control vacuolar pH and K⁺ homeostasis to regulate growth, flower development, and reproduction. *Plant Cell.* **2011**, *23*, 3482–3497. [[CrossRef](#)]
16. Zeng, Y.; Li, Q.; Wang, H.; Zhang, J.; Du, J.; Feng, H.; Blumwald, E.; Yu, L.; Xu, G. Two NHX-type transporters from *Helianthus tuberosus* improve the tolerance of rice to salinity and nutrient deficiency stress. *Plant Biotechnol. J.* **2018**, *6*, 310–321. [[CrossRef](#)]
17. Dong, H.Z.; Wang, C.M.; Xing, C.H.; Yang, T.Y.; Yan, J.X.; Gao, J.Z.; Li, D.; Wang, R.; Blumwald, E.; Zhang, S.; et al. Overexpression of *PbrNHX2* gene, a Na⁺/H⁺ antiporter gene isolated from *Pyrus betulaefolia*, confers enhanced tolerance to salt stress via modulating ROS levels. *Plant Sci.* **2019**, *285*, 14–25. [[CrossRef](#)]
18. Guan, B.; Hu, Y.Z.; Zeng, Y.L.; Wang, Y.; Zhang, F.C. Molecular characterization and functional analysis of a vacuolar Na⁺/H⁺ antiporter gene (*HcNHX1*) from *Halostachys caspica*. *Mol. Biol. Rep.* **2011**, *38*, 1889–1899.
19. Xu, K.; Zhang, H.; Blumwald, E.; Xia, T. A novel plant vacuolar Na⁺/H⁺ antiporter gene evolved by DNA shuffling confers improved salt tolerance in yeast. *J. Biol. Chem.* **2010**, *285*, 22999–23006. [[CrossRef](#)]
20. Gouiaa, S.; Khoudi, H.; Leidi, E.O.; Pardo, J.M.; Masmoudi, K. Expression of wheat Na⁺/H⁺ antiporter *TNHSX1* and H⁺-pyrophosphatase *TVP1* genes in tobacco from a bicistronic transcriptional unit improves salt tolerance. *Plant Mol. Biol.* **2012**, *79*, 137–155. [[CrossRef](#)]
21. Pandey, S.; Patel, M.K.; Mishra, A.; Jha, B. In planta transformed cumin (*Cuminum cyminum* L.) plants, overexpressing the *SbNHX1* gene showed enhanced salt endurance. *PLoS ONE* **2016**, *11*, e0159349. [[CrossRef](#)]
22. Li, C.; Wei, Z.W.; Liang, D.; Zhou, S.S.; Li, Y.H.; Liu, C.H.; Ma, F.W. Enhanced salt resistance in apple plants overexpressing a *Malus* vacuolar Na⁺/H⁺ antiporter gene is associated with differences in stomatal behavior and photosynthesis. *Plant Physiol. Biochem.* **2013**, *70*, 164–173. [[CrossRef](#)]
23. Li, Y.H.; Zhang, Y.Z.; Feng, F.J.; Dong, L.; Cheng, L.L.; Ma, F.W.; Shi, S.G. Overexpression of a *Malus* vacuolar Na⁺/H⁺ antiporter gene (*MdNHX1*) in apple rootstock M.26 and its influence on salt tolerance. *Plant Cell Tissue Organ Cult.* **2010**, *102*, 337–345. [[CrossRef](#)]
24. Geng, J.J.; Wei, T.L.; Wang, Y.; Huang, X.S.; Liu, J.H. Overexpression of *PtrbHLH*, a basic helix-loop-helix transcription factor from *Poncirus trifoliata*, confers enhanced cold tolerance in pummelo (*Citrus grandis*) by modulation of H₂O₂ level via regulating a CAT gene. *Tree Physiol.* **2020**, *39*, 2045–2054. [[CrossRef](#)]
25. Geng, J.J.; Liu, J.H. The transcription factor *CsbHLH18* of sweet orange functions in modulation of cold tolerance and homeostasis of reactive oxygen species by regulating the antioxidant gene. *J. Exp. Bot.* **2018**, *69*, 2677–2692. [[CrossRef](#)]
26. Miller, G.; Suzuki, N.; Ciftci-Yilmaz, S.; Mittler, R. Reactive oxygen species homeostasis and signalling during drought and salinity stresses. *Plant Cell Environ.* **2010**, *33*, 453–467. [[CrossRef](#)]
27. Pitzschke, A.; Djamei, A.; Bitton, F.; Hirt, H. A major role of the MEKK1-MKK1/2-MPK4 pathway in ROS signalling. *Mol. Plant* **2009**, *2*, 120–137. [[CrossRef](#)]
28. Yang, Y.Q.; Yan, G. Elucidating the molecular mechanisms mediating plant salt: Tress responses. *New Phytol.* **2017**, *217*, 523–539. [[CrossRef](#)]
29. Zhang, W.W.; Meng, J.J.; Xing, J.Y.; Yang, S.; Wan, S.B. The K⁺/H⁺ antiporter AhNHX1 improved tobacco tolerance to NaCl stress by enhancing K⁺ retention. *J. Plant Biol.* **2017**, *60*, 259–267. [[CrossRef](#)]
30. Tuteja, N. Mechanisms of high salinity tolerance in plants. *Method Enzymol.* **2007**, *428*, 419–438.
31. Xiong, L.M.; Schumaker, K.S.; Zhu, J.K. Cell signaling during cold, drought, and salt stress. *Plant Cell* **2002**, *14*, 65–83. [[CrossRef](#)]
32. Chen, C.; Chen, H.; Zhang, Y.; Thomas, H.; Frank, M.; He, Y.; Xia, R. TBtools, a toolkit for biologists integrating various biological data handling tools with a userfriendly interface. *Mol Plant* **2020**, *13*, 1194–1202. [[PubMed](#)]
33. Livak, K.J.; Schmittgen, T.D. Analysis of relative gene expression data using real-time quantitative PCR and the 2^{-ΔΔct} method. *Methods* **2002**, *25*, 402–408. [[CrossRef](#)] [[PubMed](#)]
34. Bai, L.; Ma, X.; Zhang, G.; Song, S.; Zhou, Y.; Gao, L.; Miao, Y.; Song, C.-P. A receptor-like kinase mediates ammonium homeostasis and is important for the polar growth of root hairs in *Arabidopsis*. *Plant Cell.* **2014**, *26*, 1497–1511. [[CrossRef](#)]
35. Khaskheli, A.J.; Ahmed, W.; Ma, C.; Zhang, S.; Liu, Y.Y.; Li, Y.Q.; Zhou, X.; Gao, J. *RhERF113* functions in ethylene-induced petal senescence by modulating cytokinin content in rose. *Plant Cell Physiol.* **2018**, *59*, 2442–2451. [[CrossRef](#)]
36. Tian, J.; Pei, H.X.; Zhang, S.; Chen, J.; Chen, W.; Yang, R.; Meng, Y.; You, J.; Gao, J.; Ma, N. TRV-GFP: A modified Tobacco rattle virus vector for efficient and visualizable analysis of gene function. *J. Exp. Bot.* **2014**, *65*, 311–322. [[CrossRef](#)] [[PubMed](#)]
37. Li, Z.Y.; Chen, W.; Zhang, C.; Du, C.X.; Shao, G.Y.; Cui, Y.Y. *RcMYBPA2* of *Rosa chinensis* functions in proanthocyanidin biosynthesis and enhances abiotic stress tolerance in transgenic tobacco. *Plant Cell Tissue Organ Cult.* **2019**, *137*, 441–454. [[CrossRef](#)]

38. Liu, J.H.; Inoue, H.; Moriguchi, T. Salt stress-mediated changes in free polyamine titers and expression of genes responsible for polyamine biosynthesis of apple in vitro shoots. *Environ. Exp. Bot.* **2008**, *62*, 28–35. [[CrossRef](#)]
39. Zhang, M.; Zhang, G.Q.; Kang, H.H.; Zhou, S.M.; Wang, W. *TaPUB1*, a putative E3 ligase gene from wheat, enhances salt stress tolerance in transgenic *Nicotiana benthamiana*. *Plant Cell Physiol.* **2017**, *58*, 1673–1688. [[CrossRef](#)]
40. Luo, P.; Li, Z.Y.; Chen, W.; Xing, W.; Yang, J.; Cui, Y.Y. Overexpression of *RmICE1*, a bHLH transcription factor from *Rosa multiflora*, enhances cold tolerance via modulating ROS levels and activating the expression of stress-responsive genes. *Environ. Exp. Bot.* **2020**, *178*, 104160. [[CrossRef](#)]

Disclaimer/Publisher’s Note: The statements, opinions and data contained in all publications are solely those of the individual author(s) and contributor(s) and not of MDPI and/or the editor(s). MDPI and/or the editor(s) disclaim responsibility for any injury to people or property resulting from any ideas, methods, instructions or products referred to in the content.